Sensors and Actuators A 160 (2010) 141–146

Contents lists available at ScienceDirect

Sensors and Actuators A: Physical

journal homepage: www.elsevier.com/locate/sna

A self-priming, roller-free, miniature, peristaltic pump operable with a single, reciprocating actuator

Viktor Shkolnikov[a], John Ramunas[b], Juan G. Santiago[a,*]

[a] Department of Mechanical Engineering, Stanford University, Stanford, CA 94305, USA
[b] Department of Neuroscience, Stanford University, Stanford, CA 94305, USA

ARTICLE INFO

Article history:
Received 29 September 2009
Received in revised form 26 March 2010
Accepted 21 April 2010
Available online 5 May 2010

Keywords:
Peristaltic pump
Micropump
Miniature pump
Biocompatible pump
Self-priming
Plastic pump

ABSTRACT

We present a design for a miniature self-priming peristaltic pump actuated with a single linear actuator, and which can be manufactured using conventional materials and methods. The pump is tolerant of bubbles and particles and can pump liquids, foams, and gases. We explore designs actuated by a motor (in depth) and a shape memory alloy (briefly); and briefly present a manually actuated version. The pump consists of a Delrin acetal plastic body with two integrated valves, a flexible silicone tube, and an actuator. Pumping is achieved as the forward motion of the actuator first closes the upstream valve, and then compresses a section of the tube. The increased internal pressure opens a downstream burst valve to expel the fluid. Reduced pressure in the pump tube allows the downstream valve to close, and removal of actuator force allows the upstream valve and pump tube to open, refilling the pump. The motor actuated design offers a linear dependence of flow rate on voltage in the range of 1.75–3 V. Flow rate decreases from 780 μl/min with increasing back pressure up to the maximum back pressure of 48 kPa. At 3 V and minimum back pressure, the pump consumes 90 mW. The shape memory alloy actuated design offers a 5-fold size and 4-fold weight reduction over the motor design, higher maximum back pressure, and substantial insensitivity of flow rate to back pressure at the cost of lower power efficiency and flow rate. The manually actuated version is simpler and appropriate for applications unconstrained by actuation distance.

1. Introduction

A variety of micron- and millimeter-scale fluidic device designs such as chemical analysis and drug delivery systems require miniature fluid pumps. Miniature pumps have been widely studied and are reviewed in [1,2] together with associated applications. For many applications, an ideal miniature pump would supply sufficient flow rate and pressure, while having a low voltage requirement, low power consumption, a simple control system, and low cost. We here present a miniature peristaltic pump which is potentially competitive with respect to most or all of these criteria.

Peristaltic pumps move fluid by exerting forces on the outside of a pumping chamber [2], which often consists of a flexible tube containing the fluid. Many peristaltic pumps have the advantage that the pump actuator components do not touch the fluid and that the pumping chamber can be made disposable [3] to ensure sterility and prevent cross-contamination. Miniature peristaltic pumps have been microfabricated using polydimethylsiloxane (PDMS) [4], PDMS bonded to glass [5,6], or glass bonded to silicon [7,8]. In most of these, a series of two or more actuators compress regions of a channel (the pumping chamber) to produce a peristaltic wave [3–9]. In other miniature peristaltic designs, the pump chamber is created from a section of flexible tubing and the pumping action is created by motor-driven rollers [10], magnetic balls [11], or drops of magnetic liquid [12] which compress the tube.

Here we describe a novel miniature peristaltic pump which uses a single reciprocating actuator motion to produce pumping. This pump uses off-the-shelf tubing and can be manufactured using conventional materials and methods including injection molding, stereolithography, or CNC machining.

We present in detail a version of the pump where the required linear actuation motion is achieved using a small commercial gear motor and a cam. We also briefly describe two other designs, with one actuated via shape memory alloy (SMA) wire and the other actuated manually. The motor actuated pump achieves high flow rates (0.8 ml/min) and can operate under relatively high back pressures of up to 48 kPa. The latter values are on par with or higher than many miniature pump devices [1,2]. The pump is self-priming, tolerant of bubbles and particles, and can pump liquids, gases, foams, and gels. The pump consumes 90 mW of electrical power at 3 V, and allows control of flow rate by controlling voltage. Although here we present only one size of the pump, we have created smaller and

* Corresponding author. Tel.: +1 650 723 5689; fax: +1 650 723 7657.
E-mail address: juan.santiago@stanford.edu (J.G. Santiago).

0924-4247/$ – see front matter © 2010 Elsevier B.V. All rights reserved.
doi:10.1016/j.sna.2010.04.018

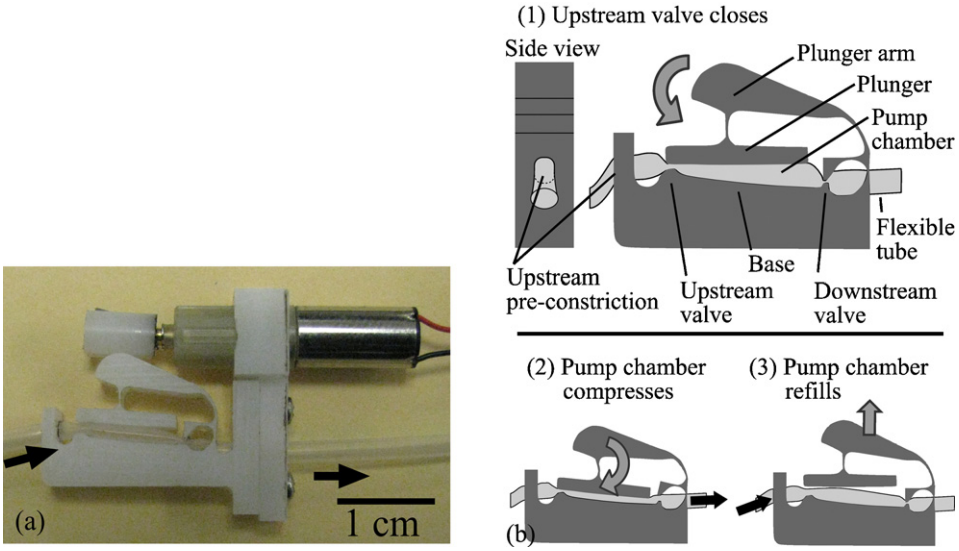

Fig. 1. (a) Pump driven by a gear motor shown in phase (1) of pumping cycle. The pumping chamber and inlet and outlet connections are a single piece of commercially available silicone tubing. Arrows indicate flow direction. The pump (with motor) is 8 mm × 22 mm × 35 mm, weighs 3.6 g, and consists of four parts: motor, cam, pump body, and tube. (b) Schematics showing phases of the pumping cycle. Black arrows indicate flow direction. Phase 1: Cam (not shown) rotation pushes down on the plunger arm, pinching the tubing and creating the upstream valve. Phase 2: Further motion of the plunger arm rotates the plunger clockwise (about the protrusion of the upstream valve), compressing the pumping chamber. Increased pressure in the pumping chamber causes the downstream burst valve to open, expelling fluid from the pumping chamber. Phase 3: The downstream valve closes as pressure is reduced in the pumping chamber. As the cam rotates further, it allows the plunger arm to spring upward, and the elasticity of the tubing and line pressure open the upstream valve. The pumping chamber draws liquid through the now-open upstream valve into the pumping chamber.

larger versions which achieve 0.1× to 5× the nominal flow rate and/or higher back pressures (up to 69 kPa).

2. Description of pump

This section describes our pump design, operation, and fabrication.

2.1. Motor-driven pump design and operation

The pump is shown in Fig. 1 and consists of four stand-alone parts: the pump body, flexible tubing, cam, and motor. To describe its operation, we divide these into seven functional components: flexible tubing, plunger arm, plunger, upstream valve, downstream valve, pre-constriction, and an actuator. The actuator presented here is a DC electric gear motor with a cam. The actuator pushes down the plunger arm, forcing it to rotate counter-clockwise about its attachment to the base. This attachment is the thin (tapers down to 0.3 mm thickness), curved section of material on the right. This motion causes the plunger to pinch the tube against a protrusion in the pump base, thus forming and closing the upstream valve (Fig. 1b, Phase 1). The thin "web" between the plunger arm and plunger (which tapers down to 0.3 mm thickness) then forces the plunger arm to rotate clockwise about the protrusion in the base and push down on the pump chamber (the section of the tube under the plunger). This raises the pressure in the pump chamber until the downstream valve (a passive element where the tube is normally pinched closed at a narrow constriction integrated into the pump body as shown) opens, expelling fluid to the outlet (Fig. 1b, Phase 2). After the fluid is expelled and pressure in the pump chamber has decreased, the downstream valve closes. Further rotation of the cam removes the actuator force. The plunger then lifts off the pump chamber and upstream valve. This allows more fluid to enter the pump chamber from the inlet (Fig. 1b, Phase 3). A vertical 2.3 mm × 1.5 mm thru-slot in the pump body with the long axis arranged perpendicular to the plane in which the tubing is flattened serves as a preconstruction. This partially compresses but does not close the tube (see side view in Fig. 1b), and helps the upstream valve section spring open quickly after the pressure from the plunger arm is released. From observing high speed movies of the operation, we estimate that the tube springs back significantly faster than the pump cycle period.

The complete pumping and valving actions are created from the motion of a single linear actuator. This pumping action is therefore very different from traveling-wave-type compression caused by moving rollers in conventional peristaltic pumps. This allows for use of linear actuators with the pump (later we discuss an SMA wire actuated version). For a discussion of the cam design please see Supplementary Information. We hypothesize our design may yield longer tubing life than typical roller designs as it subjects the tube to only one deformation mode (compression); while roller-based designs subject the tubing to both compression and longitudinal stretch. Our design requires no additional valves or internal seals.

2.2. Pump fabrication

The pump body was machined in Delrin acetal plastic (McMaster-Carr, Santa Fe Springs, CA) on a Roland MDX-540 CNC Milling Machine (Roland Corp., Irvine, CA) with a 1/16 in. diameter end mill (McMaster-Carr, Santa Fe Springs, CA). Silicone tubing (0.058 in. ID by 0.076 in. OD, VWR International, West Chester, PA) was threaded through the pump. A DC electric gear motor (gizmoszone.com, Gizmo's zone, GH6123S-B, Yuen Long, Hong Kong) with a custom-CNC-machined cam (Delrin acetal plastic, see Supplementary Information document) was attached to the pump as shown in Fig. 1a.

We chose Delrin acetal plastic as the pump body material because it is self-lubricating [13] and so reduces friction between the cam and plunger arm, and between the plunger and the silicone tubing. We note however, that we did not observe significant wearing or heating of the contact area between cam and plunger arm. Delrin has satisfactory elasticity, which allowed us to make flexing sections (e.g., between plunger arm and base), and fatigue properties. We chose silicone tubing because of its elasticity, chemical inertness, and satisfactory resistance to wear. For a discussion of our motor selection criteria please see

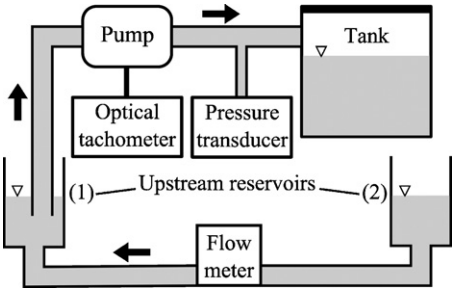

Fig. 2. Schematic of setup to quantify pump pressure, flow rate, and power performance. The pump draws liquid from one of two identical upstream liquid reservoirs 1 and 2. Arrows indicate flow direction. The flow meter section resistance is negligible so the level in both reservoirs is approximately equal. This insures that only half the flow rate withdrawn by the pump passes through the flow meter. This arrangement acts as a capacitive low-pass flow filter which filters out unsteadiness through the flow meter. The pump pumps into a closed tank, causing a steady increase in back pressure monitored by a pressure transducer. For experiments with minimal back pressure, this downstream container is opened to atmosphere. The flow meter outputs an electronic signal, and the rotational velocity of the motor shaft is monitored by an optical tachometer.

Supplementary Information. The pump with motor has dimensions 8 mm × 22 mm × 35 mm and weighs 3.4 g. The pump body dimensions are 5 mm × 12 mm × 17 mm and weighs 0.75 g. The pump assembly including a 9 cm length of tubing, pump, and motor weighs 3.6 g.

3. Experimental setup

Fig. 2 shows the measurement setup. We measured the flow rate using a Sensirion ASL 1600-20 liquid flow meter (Sensirion Inc., Westlake Village, CA) connected between two open, identical reservoirs 1 and 2 (each with 15.9 mm inner diameter) filled with deionized water and exposed to atmospheric pressure. The pump draws water directly from reservoir 1. A negligible pressure difference is required to cause flow from reservoir 2 to 1 and to maintain approximately equal liquid levels in both reservoirs. The reservoirs have identical geometry and so measured flow rate is one-half of the flow rate flowing through the pump. We used this measurement setup to avoid unsteady pulsations (order 1 s or faster time scales) in the flow meter. A similar, two-tank experimental configuration to quantify flow rate was used by Strickland [14] for a study on fuel cell water management.

We measured the pressure downstream of the pump using an Omega Engineering PX303-015G5V pressure transducer (Omega Engineering Inc., Stamford, CT) interfaced with a National Instruments NI PCI-6221 DAQ and LABVIEW Software (National Instruments, Austin, TX). The DC electric motor was typically driven by a Keithley SourceMeter 2410 power supply (Keithley Instruments Inc., Cleveland, OH) while simultaneously monitoring flow rate dependence on driving voltage and back pressure. For the power consumption experiments (cf. main plot of Fig. 5), we powered the DC motor with a Hewlett-Packard E3631A power supply. We operated the pump at constant voltage, and measured current with the respective power supply interfaced with LABVIEW Software. We measured the motor speed with an optical non-contact tachometer (Neiko Tools USA—eToolsCity, Walnut, CA).

In the flow rate and power consumption measurements of Fig. 3, we operated the pump for 2 min per voltage step and show here the middle 30 s of each data series of flow rate and electrical current (to reject transients associated with pumping and filter instrument noise). For the measurements of Fig. 4, flow rate and pressure were recorded continuously as back pressure increased. The data was then divided into 20 s segments and the time average pressure and flow rate for each segment is plotted. For the experiments associated with the main plot of Fig. 5, we present data based on 2 min time averages of electrical current.

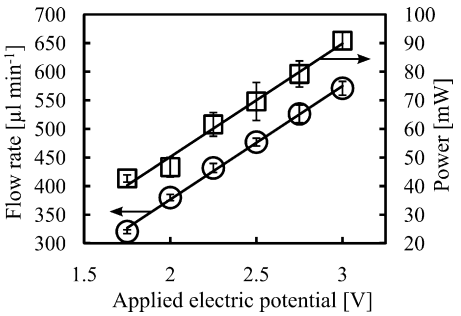

Fig. 3. Flow rate (○) and power (□) measured versus driving voltage with minimal back pressure. There is a linear relationship (R^2 = 0.998) between flow rate and voltage, which allows for convenient voltage control of flow rate. There is also a linear relationship (R^2 = 0.987) between power consumption and driving voltage. Uncertainty bars are ±1.0 standard deviation from the mean across N = 5 repetitions.

4. Results and discussion

4.1. Flow rate dependence on driving voltage and back pressure

We measured flow rate as a function of driving voltage and back pressure. Fig. 3 shows the measured flow rate at driving voltages in range of 1.75–3 V. 3 V was the maximum rated voltage of the gear motor, and 1.75 V was approximately the lowest voltage which would start the motor. We performed experiments with motor driving voltages of up to 5 V, but found voltages over 3 V caused motor overheating and rapid wear of gears. Flow rate increased linearly with increasing driving voltage against a constant back pressure. As an example, we show this trend in Fig. 3 for the case of negligible back pressure.

Pump flow rate was equal to the product of stroke volume (net volume of liquid expelled in one cycle) and stroke rate. We found a pump's stroke volume was mainly controlled by pump geometry and materials (e.g., tubing diameter, plunger dimensions). For a constant back pressure, we found stroke volume was approximately independent of driving voltage. For a DC electric motor with approximately constant armature resistance and supplying back-e.m.f., motor speed ω is related to driving voltage as follows [15]:

$$\omega = \frac{V - R_a(T/K_T)}{K_E}, \quad (1)$$

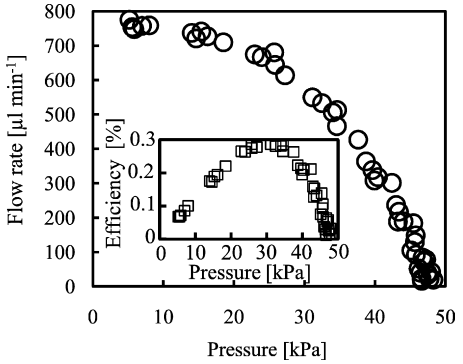

Fig. 4. Pump flow rate (○) as a function of back pressure. Flow rate decreases gradually with increasing back pressure (from a maximum value of 780 μl/min), as expected. The motor was operated at 3 V, and the maximum pressure achieved was 48 kPa. The inset plot shows thermodynamic efficiency (□) as a function of back pressure. A maximum efficiency 0.3% is reached at a back pressure of 30 kPa.

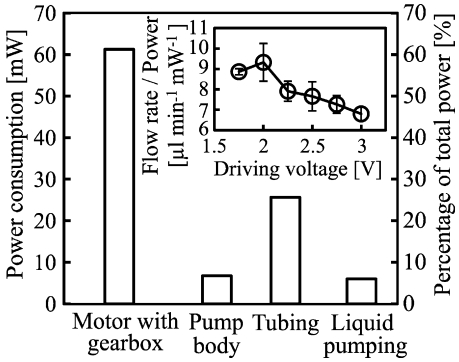

Fig. 5. Breakdown of power consumption by component. The total power consumed by pump at 3 V and 30 kPa back pressure (the maximum thermodynamic efficiency point) is 100 mW. The motor and gearbox consume most of the power (61%); compression of the tubing consumes 26%; and compression of elastic joints and movement of the plunger arm (pump body) 7%. Additional power consumed to pump deionized water accounts for only 6% of total power. The inset shows a plot of flow rate per power consumed versus driving voltage against minimal back pressure. Flow rate per power decreases with driving voltage, leading to lower efficiency at higher voltages. Uncertainty bars are ±1.0 standard deviation from the mean ($N = 5$).

where V is driving voltage, R_a is armature resistance, T is torque produced, K_T is the motor's torque constant, and K_E is the motor's back-e.m.f. constant. Three types of forces contribute to time-averaged torque: elastic spring force associated with compressing the fluid-filled tube and bending of the flexible pump body; inertial forces associated with accelerating plunger arm and working fluid; and damping effects of the fluid and pump body. We estimate an elastic force of 2 N by measuring the force required to actuate the plunger arm with air in the pump using a scale (Pinnacle PI-225D, Denver Instruments, Denver, CO). In contrast, the inertial force required to actuate the pump is order 2×10^{-4} N (using mass of the plunger arm and tube section and the observed time scales). The inertial force associated with moving the 20 μl of fluid through 7 mm distance in less than 1 s is order 3×10^{-7} N (the maximum instantaneous Reynolds number based on tube diameter and maximum flow velocity is ~20, the product of Reynolds and Strouhal numbers with Strouhal number based on 1 s pumping period, tube diameter, and maximum velocity was ~7). We hypothesize the elastic force also dominates the damping forces (in pumping water or air). Such dominant elastic force yields approximately constant torque and, from Eq. (1), we see this implies a linear relationship between ω and T. This likely explains the observed (convenient) linear trend between flow rate and applied voltage.

Fig. 4 shows measured flow rate as a function of pump back pressure for operation at 3 V. Flow rate decreases from 780 μl/min with increasing back pressure up to the maximum back pressure of 48 kPa. Motor speed (and stroke rate) was observed to vary less then 2% throughout the experiment. The decrease in flow rate with increasing back pressure is likely due to a decrease in net stroke volume. We attribute this to increased intermittent back flows through the downstream valve. These likely occur near the beginning of Phase 3 in Fig. 1. This hypothesis is supported by observations we made of a meniscus in the downstream tube. We observed this meniscus moved slightly upstream with each pump cycle, and that the intermittent upstream motion increased with increasing back pressure.

We note that in addition to pumping against higher than atmospheric back pressure, the pump can pump against and create a vacuum. For example, we performed limited experiments (not shown here) where we used the pump to evacuate water from a 15 ml chamber. We reduced this chamber's pressure to about 13 kPa below atmospheric (−13 kPa gage).

4.2. Design variations of the motor-driven pump

We explored ~50 variations of the design shown in Fig. 1. This included various plunger arm geometries, valve designs, tubing types, and pre-constriction designs. Here we offer comments which may be helpful in future efforts. Reproducibility across pumps of a single design is strongly influenced by machining and/or molding tolerances. The upstream valve design is fairly robust to geometric variations. However, the downstream valve design is very sensitive to geometric variations (we report here on our best design). The cam should be large enough to allow travel of the plunger arm for sufficient stroke volume, but overly large cams require excessive torque and stall the motor. Stiffer (tighter tube pinch) downstream valves yield higher pump pressure capacity and less sensitivity to back pressure (indeed, we created designs where flow rate is largely insensitive to back pressure throughout the lower ~70% of the pressure range). We hypothesize that pump pressure can be increased by increasing output motor torque and slightly increasing tube stiffness. However, overly stiff downstream valves show lower and less reproducible flow rate and cause other problems. For example, we found high burst pressure downstream valves are strongly correlated with bubble formation in the pump. The bubble formation leads to inconsistencies in net stroke volume and thus inconsistencies in flow rate. We hypothesize such valves cause a finite time (between Phases 2 and 3) where both valves are closed and the opening of the pump chamber significantly lowers pressure in the pump chamber. This likely causes degassing (and, less likely, vaporization/cavitation) and bubble creation.

4.3. Efficiency and power consumption

We define the pump's thermodynamic efficiency η in the usual manner as,

$$\eta = \frac{pQ}{VI}, \tag{2}$$

where p is the back pressure, Q is the flow rate, V is the driving voltage, and I is the current drawn. The thermodynamic efficiency of this pump peaks at 0.3% at a back pressure of 30 kPa, as shown in the inset of Fig. 4. Although obviously much lower than traditional macro-scale pumps, this thermodynamic efficiency is on the same order as (or better than) many microscale and miniature pumps. For example, Chen and Santiago report maximum thermodynamic efficiencies of 0.5% for miniature planar electroosmotic pumps [16]; while Sim et al. report performance corresponding to a thermodynamic efficiency of 4×10^{-7}% for a phase change diaphragm pump [17]. We estimate the miniature peristaltic pump Instech P625/275, commercialized by Instech Laboratories Inc., has a maximum thermodynamic efficiency of roughly 0.2% [18].

Fig. 5 shows estimates of the power consumption of each pump component for operation at 22 °C and 3 V against 30 kPa back pressure (maximum thermodynamic efficiency point). The data were obtained from measurements on the motor and gear box alone (case 1); the motor, gear box, and attached pump body (case 2); the complete assembly pumping air (case 3); and the complete assembly pumping liquid (case 4). The estimates shown for the second through fourth bars are obtained by subtracting the power of case 1 from case 2; case 2 from case 3; and case 3 from case 4.

For the current choice of motor for this pump, the motor and gearbox consume over 60% of the power, while the power to pump water is only ~6% of total power. Total power consumption as a function of driving voltage, against minimal back pressure, is shown in Fig. 3. Total power consumption increases linearly with increasing driving voltage. However, flow rate per power ratio (Fig. 5 inset) mostly decreases with driving voltage and so efficiency decreases at higher voltages. The large fraction of power consumed by the

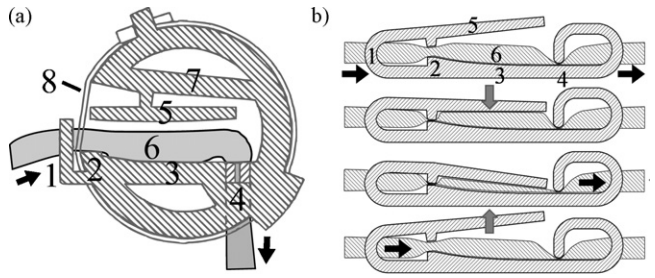

Fig. 6. Miniature peristaltic pumps with two alternate actuation modalities: SMA wire actuated (a) and manualy actuated pump (b). Black arrows signify the direction of flow. (a) SMA wire actuated pump consists of eight major components: 1. pre-constriction, 2. upstream valve, 3. base, 4. downstream valve, 5. plunger, 6. pumping chamber (flexible tube), 7. plunger arm, and 8. SMA wire (actuator). We achieved an approximately 5-fold size reduction over the motorized pump using shape memory alloy wire as an actuator. (b) A manually actuated version of the design with only a plunger (and no plunger arm), and which requires greater actuator travel. Gray arrows indicate plunger motion. The pump consistist of six major components: 1. pre-constriction, 2. upstream valve, 3. base, 4. downstream valve, 5. plunger, and 6. pumping chamber (flexible tube).

actuator suggests there is room for improvement in the choice of actuator.

4.4. Pumping other media

We performed additional flow measurements which demonstrate pumping of gases, foams, suspensions, and liquids with higher and lower viscosity than water. Table 1 summarizes results for a variety of media pumped (with minimal back pressure and at 3 V). We measured the flow rate of glycerol (Mallinckrodt, Hazelwood, MO) and mild foam hand soap (DigiClean, Ecolab, St. Paul, MN) by measuring the speed of the fluid meniscus in a thin graduated tube. We measured the flow rate of methanol (99.8%, Fisher Scientific Inc., Pittsburgh, PA) and the alumina (Alfa Aesar, Ward Hill, MA) suspension, by measuring the time to pump a certain weight of the fluid into a tank on the Pinnacle scale described earlier. Air flow rate was measured using a digital flow meter (Intelligent Digital Flow Meter, Varian Analytical Instruments, Palo Alto, CA).

4.5. SMA and manually actuated versions of the pump

We developed and tested two other pump actuator modalities. The first is actuated with shape-memory alloy (SMA) wire and the second can be actuated manually (by hand). We provide here a very brief description of these designs.

The SMA wire actuated pump is shown schematically in Fig. 6a (see Supplementary Information for more details and movie of operation). This design operates in a manner similar to the motor actuated design, except the depression and relaxation of the plunger arm is brought about by heating and cooling of the SMA wire, actuated with a square-wave voltage source (causing it to contract and relax). We used a 100 mm length of 0.005 in. diameter NiTi Flexinol SMA wire from Dynalloy, Inc. (Costa Mesa, CA) wrapped around the body of the pump, creating a peristaltic pump with only three parts (pump body, flexible tube, and SMA wire). This design achieved 5-fold package volume and 4-fold weight reductions over the motor design. We wrap the pump body with a single SMA wire in two loops to double actuation force (with equal displacement) at the cost of doubled actuator power. Details regarding its operation are summarized in Table 2 and compared to parameters of the motorized version. Additional information of this SMA actuated design (including a video) is given in Supplementary Materials.

We also tested a simpler design which employs just the plunger without an additional plunger arm (see Fig. 6b). This design is intended for situations where travel distance of the actuator is not a constraint, as in manual actuation. As with the motorized design, the depression of the plunger closes the upstream valve, preventing upstream fluid flow. As the plunger depresses further, it compresses and raises pressure in the pumping chamber. This increase in pressure opens the downstream burst valve. Once fluid is expelled, the downstream valve closes. As the plunger is raised, the upstream valve opens and fluid fills the pumping chamber from upstream. We include additional details of this design (including a video of operation) in Supplementary Materials.

Table 1
Motor-driven pump flow rate performance with selected media.

Media pumped	Flow rate (μl/min)
Deionized water	780
Glycerol (~500 cP)	18
Methanol (~0.5 cP)	530
Suspension of 40–50 nm alumina particles in deionized water (1:20 by weight)	800
Mild foam hand soap	900
Atmospheric air at 22 °C	2500

Table 2
Summary of figures of merit for motor and SMA wire actuated pump designs.

Figure of merit	SMA wire actuated pump	Motor actuated pump
Operating voltage	4 V	1.75–3 V
Nominal voltage	4 V	3 V
Power consumption	420 mW	40–90 mW
Flow rate range	0–60 μl/min	0–780 μl/min
Maximum flow rate/power	0.1 $\mu l\,min^{-1}\,mW^{-1}$	9 $\mu l\,min^{-1}\,mW^{-1}$
Operating pressure	0–69 kPa	0–48 kPa
Package volume	1.3 cm^3	6.2 cm^3
Weight	0.9 g	3.6 g
Continuous operation tested	14,400+ cycles	288,000+ cycles
Actuator	Shape memory alloy wire	DC electric gear motor with cam

5. Conclusion

We have presented a miniature peristaltic pump design which can use a single (linear) actuator motion to effect both valving and pumping actions. We described motor, SMA, and manually actuated versions of the design. The pump is self-priming, tolerant of bubbles and particles, can pump liquids, foams, and gases, and can be manufactured using conventional materials and methods such as injection molding or CNC machining. All designs presented here were fabricated from Delrin acetal plastic and a flexible silicone tube acts as the pump chamber.

The motor actuated pump's flow rate is linearly dependent on driving voltage in the range of 1.75–3 V against a constant back pressure, allowing for easy regulation of flow rate. Pump flow rate decreases from 780 μl/min with increasing back pressure up to the maximum back pressure of 48 kPa. The pump consumes ~90 mW of power, pumping against minimal back pressure at 3 V. However, we estimate only 6% of this power is used to drive the liquid while over 60% of the power is consumed by the motor and gearbox, motivating improvement in the choice of the actuator. This pump system measures 8 mm × 22 mm × 35 mm and weighs 3.6 g.

The SMA actuated pump offers lower flow rates (a maximum of 60 μl/min) and lower flow rate per power (0.14 $\mu l\,min^{-1}\,mW^{-1}$). However, it offers a 5-fold package volume reduction and 4-fold weight reduction over the motor actuated pump, and allows for further downscaling. The manually actuated design is simpler and intended for situations where travel distance of actuator is not a design constraint.

In future work we hope to further develop the SMA design and study long-term performance, reliability, reproducibility (manufacturing), and power consumption.

Acknowledgements

We gratefully acknowledge support from the Department of Defense under contract number W81XWH-07-1-0384. V.S. was supported by Stanford VPUE FGUR grant. J.R. was supported by a National Sciences and Engineering Research Council of Canada Postgraduate Scholarship and the Lucille P. Markey Biomedical Research Fellowship.

Appendix A. Supplementary data

Supplementary data associated with this article can be found, in the online version, at doi:10.1016/j.sna.2010.04.018.

References

[1] D.J. Laser, J.G. Santiago, A review of micropumps, J. Micromech. Microeng. 14 (2004) R35–R64.
[2] B.D. Iverson, S.V. Garimella, Recent advances in microscale pumping technologies: a review and evaluation, Microfluid Nanofluid 5 (2008) 145–174.
[3] N.J. Graf, M.T. Bowser, A soft-polymer piezoelectric bimorph cantilever-actuated peristaltic micropump, Lab Chip 8 (2008) 1664–1670.
[4] W. Mamanee, A. Tuantranont, N.V. Afzulpurkar, N. Porntheerapat, S. Rahong, A. Wisitsoraat, PDMS based thermopneumatic peristaltic micropump for microfluidic systems, J. Phys.: Conf. Ser. 34 (2006) 564–569.
[5] O.C. Jeong, S.W. Park, S.S. Yang, J.J. Pak, Fabrication of a peristaltic PDMS micropump, Sens. Actuators A 123–124 (2005) 453–458.
[6] J.M. Berg, R. Anderson, M. Anaya, B. Lahlouh, M. Holtz, T. Dallas, A two-stage discrete peristaltic micropump, Sens. Actuators A 104 (2003) 6–10.
[7] L.-S. Jang, Y.-J. Li, S.-J. Lin, Y.-C. Hsu, W.-S. Yao, M.-C. Tsai, C.-C. Hou, A stand-alone peristaltic micropump based on piezoelectric actuation, Biomed. Microdev. 9 (2007) 185–194.
[8] D. Lee, J.S. Koa, Y.T. Kim, Bidirectional pumping properties of a peristaltic piezoelectric micropump with simple design and chemical resistance, Thin Solid Films 468 (2004) 285–290.
[9] J. Xie, J. Shih, Q. Lin, B. Yangb, Y. Taia, Surface micromachined electrostatically actuated micro peristaltic pump, Lab Chip 4 (2004) 495–501.
[10] C. Koch, V. Remcho, J. Ingle, PDMS and tubing-based peristaltic micropumps with direct actuation, Sens. Actuators B 135 (2009) 664–670.
[11] M. Du, X. Ye, K. Wu, Z. Zhou, A peristaltic micro pump driven by a rotating motor with magnetically attracted steel balls, Sensors 9 (2009) 2611–2620.
[12] E. Kim, J. Oh, B. Choi, A study on the development of a continuous peristaltic micropump using magnetic fluids, Sens. Actuators A 128 (2006) 43–51.
[13] Delrin Design Guide—Module III, 1997, http://plastics.dupont.com/plastics/pdflit/americas/delrin/230323c.pdf.
[14] D.G. Strickland, Personal communication, 2009.
[15] T. Kenjo, S. Nagamori, Permanent-Magnet and Brushless DC Motors, Oxford University Press, 1985, pp. 6–8.
[16] C.-H. Chen, J.G. Santiago, A planar electroosmotic micropump, J. Micromech. Syst. 11 (6) (2002) 672–683.
[17] W.Y. Sim, H.J. Yoon, O.C. Jeong, S.S. Yang, A phase-change type micropump with aluminum flap valves, J. Micromech. Microeng. 13 (2003) 286–294.
[18] Setup Instructions P625 Peristaltic Pumps, 2004, http://www.instechsolomon.com/Support/manuals/P625manual.pdf.